Duality-Synthesized Circuit for Eddy Current Effects in Transformer Windings

Saeed Jazebi, *Student Member, IEEE*, Francisco de León, *Senior Member, IEEE*, and Behrooz Vahidi, *Senior Member, IEEE*

***Abstract*—This paper presents a novel method to obtain an equivalent circuit for the modeling of eddy current effects in the windings of power transformers. The circuit is derived from the principle of duality and, therefore, matches the electromagnetic physical behavior of the transformer windings. It properly models the flux paths and current distribution from dc to MHz. The model is synthesized from a nonuniform concentric discretization of the windings. Concise guidelines are given to optimally calculate the width of the subdivisions for various transient simulations. To compute the circuit parameters only information about the geometry of the windings and their material properties is needed. The calculation of the circuit parameters does not require an iterative process. Therefore, the parameters are always real, positive, and free from convergence problems. The results are compared with conventional synthesis methods and finite elements for validation.**

***Index Terms*—Eddy currents, electromagnetic transients, principle of duality, skin effect, transformer modeling.**

I. Introduction

EDDY CURRENTS induced during high-frequency transients in power transformers cause nonuniform distribution of the magnetic flux in the iron core and nonuniform current distribution in the windings. Eddy current losses in transformer cores are conventionally represented, for steady-state studies (50/60 Hz) by a constant resistor in parallel with a magnetizing inductor, and dynamic eddy currents in the windings are neglected. Obviously, the constant resistance model is meant for steady-state analysis and not for transient studies. Therefore, this model is not accurate for many types of transient studies. Mid-frequency, high-frequency, and even some low-frequency studies (for example, ferroresonance), require accurate representation of the frequency-dependent effects of eddy currents in the windings and in the core.

The goals of modeling eddy current effects are to properly represent the eddy losses and the nonuniform distribution of the leakage flux within the transformer windings. A common method to obtain a high-frequency transformer model is to replace lumped leakage inductances by ladder-type $(R-L)$ equivalent circuits [1]–[11]. There are two main steps to synthesize a realizable equivalent circuit: 1) choosing a proper model configuration compatible with the frequency response of the winding and 2) the accurate calculation of the circuit parameters. Currently, there is no optimum-order fully dual model for transformer windings that in addition to matching the terminal behavior, can be built using only elements already available in the Electromagnetic Transients Prgram (EMTP)-type programs. The next section presents a detailed literature review of existing publications in this area.

The main contribution of this paper is to produce a high-frequency model for the study of eddy current effects in transformer windings that is in full compliance with the principle of duality between electric and magnetic circuits. This paper is a step forward toward achieving the final objective of creating a fully dual model for transformers, including eddy currents in the core and windings.

The high-frequency model is obtained from the analytical solution of the low-frequency electromagnetic-field problem in the windings considering the coil curvature. The model is completely dual and physically consistent. Frequency-dependent expressions for the impedance (or admittance) are not required to compute the value of the circuit parameters. Only simple expressions for low-frequency resistance and inductance are needed to construct a high-frequency model. The formulas exclusively require information about the geometry and material properties of the windings. The calculation does not rely on an iterative process; hence, the parameters are always real and positive, and the circuit is always realizable. In addition, the computational effort for obtaining the model parameters is very small and convergence problems are completely avoided.

The model order is minimized by an optimal subdivision pattern of the windings. The model is valid from dc to MHz. Concrete guidelines are given to calculate the width of the subdivisions depending on the desired frequency range. The new model is compared with the commonly used methods and against finite-element simulations. Since the model is completely dual, each node represents a physical point in the conductor. This is corroborated with simulations showing that the magnetic flux and current in each subdivision of the winding can be obtained from the electrical variables measured in the dual electrical model.

II. Literature Review

A. Available Equivalent Circuits

In circuit synthesis theory, several ladder-shaped equivalents exist for the modeling of eddy current effects [12]. Fig. 1 shows

Manuscript received June 18, 2012; revised October 18, 2012 and November 24, 2012; accepted December 28, 2012. Date of publication February 20, 2013; date of current version March 21, 2013. Paper no. TPWRD-00629-2012.

S. Jazebi and F. de León are with the Department of Electrical and Computer Engineering, Polytechnic Institute of New York University, Brooklyn, NY 11201 USA (e-mail: jazebi@ieee.org; fdeleon@poly.edu).

B. Vahidi is with the Department of Electrical Engineering, Amirkabir University of Technology, Tehran 1591634311, Iran (e-mail: vahidi@aut.ac.ir).

Color versions of one or more of the figures in this paper are available online at http://ieeexplore.ieee.org.

Digital Object Identifier 10.1109/TPWRD.2013.2238257

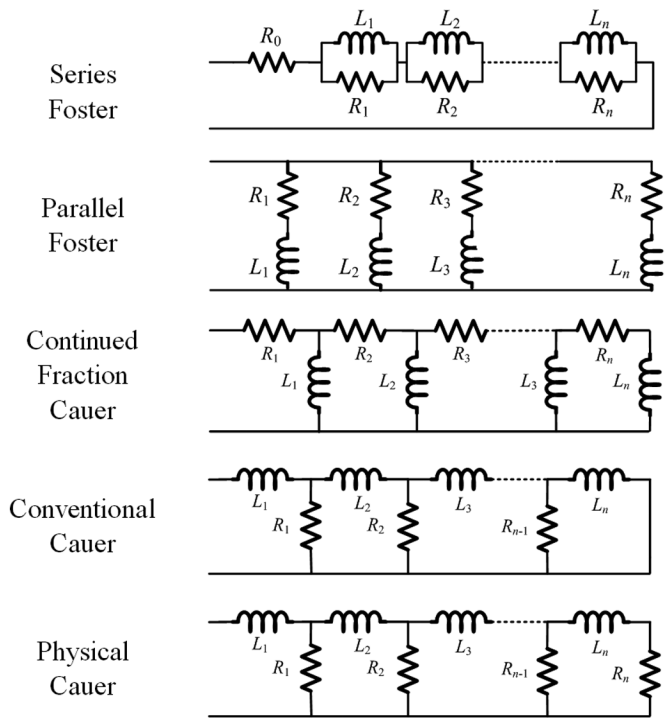

Fig. 1. Available frequency-dependent models for transformer windings.

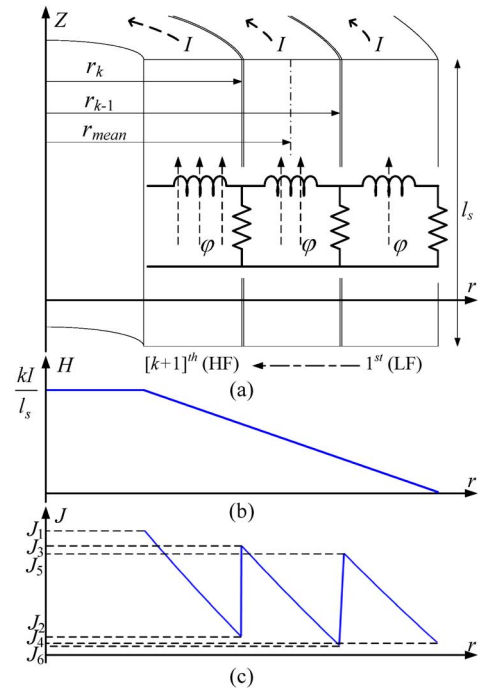

Fig. 2. (a) Illustration of the physical significance of the dual Cauer circuit for modeling eddy currents in the outer winding of a two-winding transformer (multilayer winding). (b) Magnetic field. (c) Current density distribution at $\omega = 0$. Note: HF refers to high-frequency region and LF refers to the low-frequency region.

the most common equivalent circuits used to model transformer windings.

References [1]–[5] have proposed Foster equivalent circuits to model eddy current effects. Foster equivalents are terminal models that are only valid for the study of the terminal behavior. For example, they are not capable of physically representing the nonlinearities of the magnetic materials [6]. In [7]–[9], transformer windings are modeled with Cauer equivalent circuits. In [9], Holmberg, Leijon, and Wass physically derived the parameters of the Cauer model by means of the principle of duality to model skin effects in coils. (See also [10].)

Three different shapes of Cauer models exist. In this paper, these models are called Continued Fraction Cauer, Conventional Cauer, and Physical Cauer. (See Fig. 1.) The Continued Fraction Cauer is a terminal circuit similar to Foster circuits and suffers from the same disadvantages. In the Conventional Cauer and the Physical Cauer models, transversal inductors correspond in the duality sense to magnetic flux paths (or reluctances) for winding sections. The paths of eddy currents are modeled by resistors [6].

In the Conventional Cauer circuit, the impedance seen from the terminals reduces to zero when $\omega \rightarrow 0$. No induced currents exist at zero frequency in the transformer core. Thus, the Conventional Cauer model works properly, in the dual sense, for iron cores. In contrast, windings must carry current at low frequencies and even at 0 Hz. Consequently, the equivalent circuit should properly represent the resistance from dc to the highest desired frequency. The Conventional Cauer circuit is capable of representing inductances properly even at dc. However, this model fails to represent the dc resistance. At low frequencies, the resistance is dominant, but in the Conventional Cauer model, all resistors are shorted by the inductors. (See Fig. 1.) The Physical Cauer circuit fulfills the principle of duality in every aspect and precisely represents the frequency dependency. Thus, this paper proposes using the Physical Cauer for transformer windings.

Fig. 2 shows how the Physical Cauer equivalent can be derived for a multilayer winding. The figure illustrates the outer winding of a two-winding transformer. The magnetic field at the inner side is stronger than at the outer layers and decays to zero for the outmost layer. The currents in all layers are equal since they are electrically connected in series (neglecting capacitances). The current density distribution varies between the layers due to the cylindrical geometry of the winding.

According to the principle of duality, an equivalent inductor represents a flux path in substitution of the corresponding reluctance. Also, eddy currents circulating in the winding corresponding to each flux path exist. To model the current path and damping effects, resistors are included in the model between two consecutive inductive sections.

At higher frequencies, the flux density increases in the regions closer to the center of the cylinder. Thus, physically, the terminal components of the equivalent circuit represent higher frequencies and the innermost blocks represent the low frequencies. At low frequencies, the values of the resistors in the equivalent circuit are larger than the values of the reactances, resulting in a uniform distribution of the electromagnetic field within the section (except for the effect of curvature); remember that in a dual model, each resistor and inductor correspond to a subdivision of the conductor. On the other hand, as the frequency increases, the

reactances become increasingly dominant and produce nonuniform distribution of flux concentrated at the surface.

B. Calculation Techniques

Three main categories exist when computing the parameters of equivalent circuits: iterative fitting [1]–[3], [7]; mathematical continued fraction expansions [11]; and domain discretization methods [7]–[9].

In [11], the author presents a continued fraction model based on the capacitance-permeance analogy. The method uses straightforward analytical expressions to calculate the parameters. Continued fraction models do not comply with the principle of duality between electric and magnetic circuits. Hence, although they are physically sound, they are not compatible with our final modeling goal.

Iterative methods were applied for the first time in [1]. Later, the authors extracted parameters in an R-matrix to model a complete transformer [2]. Since the model cannot be built directly with elements available in EMTP-type programs, an "add-on" circuit was developed which could connect in series with any transformer model [3]. The method is very sensitive to initialization and may diverge or converge with negative inductors. In addition, the final circuit is not fully meaningful in the dual sense.

Domain discretization methods are based on the division of the physical objects into sections perpendicular to the flux paths. In these methods, parameters are calculated for each section independently. Nonuniform discretization can reduce the order of these circuits effectively. Some references propose the use of a proportionality constant to split objects exponentially [7]–[9]. To increase the model accuracy, the number of divisions should be increased or the proportionality constant must be varied. This means that the ratio cannot be assumed constant. These models are physically correct but do not guarantee a realizable optimum circuit. Also, the order of the synthesized circuits is preselected by dividing the winding into several concentric regions. The circuit order, and consequently, computational effort can be reduced by optimization.

III. Calculation of Model Parameters

In this section, the electromagnetic field equations are solved and a formula to compute the circuit elements is presented.

A. Analytical Impedance Formula

In this paper, different from most previous publications in the field, the curvature of the windings is considered since it represents the reality more closely. The winding has a cylindrical shape and thus, the field problem is solved in cylindrical coordinates; 3-D electromagnetic fields are computed with 2D axisymmetric FEM simulations. It is assumed that the magnetic field strength (H) is completely axial. Considering $H_z(r,t) = H_z(r)e^{j\omega t}$ and writing the diffusion equation in cylindrical coordinates [13], [14], we have

$$r^2\frac{\partial^2 H_z(r,t)}{\partial r^2} + r\frac{\partial H_z(r,t)}{\partial r} - j\omega\mu\sigma r^2 H_z(r,t) = 0. \quad (1)$$

Equation (1) is a Bessel-type partial differential equation [15]. Parameters $\omega, \sigma, \mu, H_z, r, t$ are angular frequency, material electrical conductivity, magnetic permeability, magnetic field strength in z direction, radial distance from the center, and time, respectively. The general solution of (1) is given by

$$H_z(r,t) = \left[C_1 J_0(\alpha r) + C_2 Y_0(\alpha r)\right] e^{j\omega t} \quad (2)$$

where $\alpha = j\sqrt{j\omega\mu\sigma}$, and J_0, Y_0 are order zero Bessel functions of the first and second kind, respectively. The boundary conditions for the outer winding of a two-winding transformer with the length l_s are

$$H_z(r_{k-1},t) = \frac{(k-1)Ie^{j\omega t}}{l_s} \text{ and } H_z(r_k,t) = \frac{kIe^{j\omega t}}{l_s}. \quad (3)$$

Thus, coefficients C_1 and C_2 in (2) become

$$C_1 = \frac{I}{l_s}\left\{\frac{(1-k)Y_0(\alpha r_k) + kY_0(\alpha r_{k-1})}{J_0(\alpha r_k)Y_0(\alpha r_{k-1}) - J_0(\alpha r_{k-1})Y_0(\alpha r_k)}\right\}$$
$$C_2 = \frac{I}{l_s}\left\{\frac{(k-1)J_0(\alpha r_k) - kJ_0(\alpha r_{k-1})}{J_0(\alpha r_k)Y_0(\alpha r_{k-1}) - J_0(\alpha r_{k-1})Y_0(\alpha r_k)}\right\} \quad (4)$$

where I, r_k are the peak current, and inner radius of the kth layer. The electric field is calculated from Maxwell Equations as

$$E_\varphi(r,t) = \frac{-1}{\sigma}\frac{\partial H_z(r,t)}{\partial r} = \frac{\alpha e^{j\omega t}}{\sigma}\left(C_1 J_1(\alpha r) + C_2 Y_1(\alpha r)\right). \quad (5)$$

Applying Poynting's theorem, the power of the kth section with an inner and outer radius r_k and r_{k-1} is given by

$$S = \frac{1}{2}\int (E \times H^*)ds = \frac{1}{2}\int_0^{2\pi}\int_0^{l_s} E_\varphi(r,t)H_z^*(r,t)rd\varphi dz$$
$$= \frac{\pi\alpha I}{\sigma}\left\{\begin{array}{l}\left[C_2 Y_1(\alpha r_k) + C_1 J_1(\alpha r_k)\right] kr_k \\ -\left[C_2 Y_1(\alpha r_{k-1}) + C_1 J_1(\alpha r_{k-1})\right](k-1)r_{k-1}\end{array}\right\}. \quad (6)$$

The simplest form of the impedance is presented in (7) at the bottom of the next page. The purpose of coefficient 2 is to convert the peak value of I to the rms value. It should be noted that the expression is also applicable to the inner winding by simply exchanging variables r_k and r_{k-1}. For high frequencies, the following asymptotic approximations can be applied [15]:

$$J_n(\alpha r) \approx \sqrt{\frac{2}{\pi\alpha r}}\cos\left[\alpha r - (2n+1)\pi/4\right]$$
$$Y_n(\alpha r) \approx \sqrt{\frac{2}{\pi\alpha r}}\sin\left[\alpha r - (2n+1)\pi/4\right]. \quad (8)$$

The simplified expression for the impedance is [1]

$$Z = \frac{2\pi\alpha}{\sigma l_s}\left[\begin{array}{c}(k^2 r_k + (k-1)^2 r_{k-1})\cot(\alpha d) \\ -2k(k-1)\sqrt{r_k r_{k-1}}\csc(\alpha d)\end{array}\right]. \quad (9)$$

Different from [1], the variable α has a multiplication by j inside; thus, (9) uses circular, rather than hyperbolic, trigonometric functions. For a single-layer winding, (9) reduces to

$$Z = \frac{[2\pi\alpha r_k \cot(\alpha d)]}{\sigma l_s} \quad (10)$$

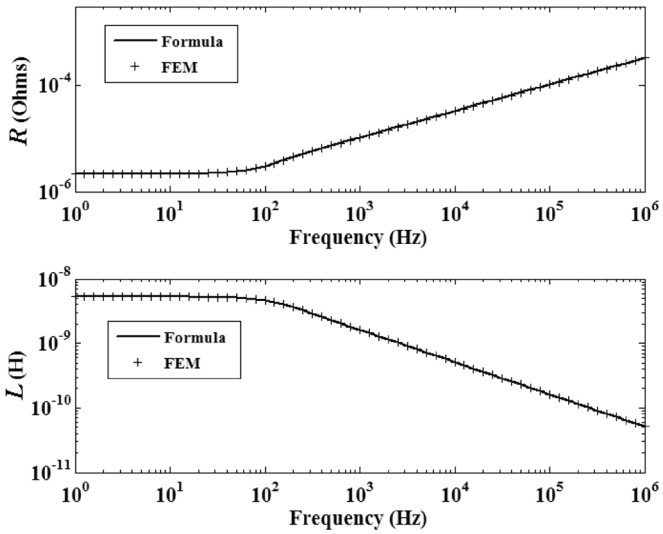

Fig. 3. Comparison of the formula (11) with FEM ($d = 1$ cm, $r_{in} = 20$ cm, $l_s = 1$ m).

which can be used to derive the continued fractions model described in the previous section. The approximate equation (10) is valid for inductance values with input parameter r_k but is not perfectly accurate for resistance values at low frequencies (error of about 5%). To properly compute the resistances, r_k should be replaced by the mean radius r_{mean}.

Then, the resistance and inductance are computed from

$$R = \mathrm{Re}\left(\frac{[2\pi\alpha r_{mean}\cot(\alpha d)]}{\sigma l_s}\right) \tag{11a}$$

$$L = \omega^{-1}\mathrm{Im}\left(\frac{[2\pi\alpha r_k\cot(\alpha d)]}{\sigma l_s}\right). \tag{11b}$$

Fig. 3 compares the values computed with the formula (11) with those from FEM. This figure shows the validity of the analytical formula. The maximum and average differences for resistance values are 2.61% and 1.5% and for inductance values, they are 0.36% and 0.04%, respectively.

B. Physical Cauer Model Parameters

Since high-frequency behavior is greatly dependent on the inductances, it is critical to derive accurate expressions for them. The following subsections describe two models that represent the winding, depending on the relative value of the thickness/frequency ratio compared with the penetration depth ($\delta = \sqrt{2/\omega\mu\sigma}$).

1) Large Penetration Depth Model: The model proposed in this paper is based on the fact that the dc behavior of a sufficiently thin subdivision of the winding closely resembles the higher-frequency response. This is so when the penetration depth is (much) larger than the thickness of the subdivision. Thus, in the equivalent circuit, we aim to model the frequency response of the winding with electromagnetic parameters near zero frequency.

For lower frequency applications, a multilayer winding can be represented by a Cauer model having only one $R-L$ block per layer. (See Fig. 2.) To calculate the parameters of this circuit, (1) is solved at low-frequency steady-state conditions $\omega \to 0$. Therefore, (1) can be reduced to the dc condition ($\omega = 0$) to become Euler's equation, which solution is given by

$$H_z(r) = \frac{kI}{l_s} + \frac{I}{l_s \ln\left(\frac{r_k}{r_{k-1}}\right)}\ln\left(\frac{r}{r_k}\right). \tag{12}$$

Then, the dc inductance for the kth layer can be calculated by integrating the magnetic energy density as follows:

$$\begin{aligned} L_{\mathrm{DC},k} &= \frac{2W}{I^2} = \int_0^{2\pi}\int_0^{l_s}\int_{r_k}^{r_{k-1}} \frac{\mu H_z^2(r) r d\varphi dr dz}{I^2} \\ &= \frac{\mu\pi r_k^2}{l_s D}\left\{\left(\frac{r_{k-1}}{r_k}\right)^2 (B^2+B+0.5) - A^2 \right. \\ &\qquad \left. + A - 0.5\right\} \end{aligned} \tag{13}$$

where

$$A = k\ln\left(\frac{r_k}{r_{k-1}}\right),\ B = (1-k)\ln\left(\frac{r_k}{r_{k-1}}\right),\ D = \ln^2\left(\frac{r_k}{r_{k-1}}\right).$$

The inductance values computed with (13) can be used directly in the equivalent circuit of Fig. 2. As described before, in this model, each layer of the winding is represented by a single R–L section. Thus, this model is only valid for low frequencies. To synthesize a model compatible with higher frequencies, a more detailed circuit is required.

2) Small Penetration Depth Model: A higher frequency model for a layer in a winding can be constructed from dc resistances and inductances as shown in Fig. 4. A single layer of the winding is divided into a number of concentric cylinders. As discussed previously, the number of ladder sections can be reduced by recognizing that as the frequency increases, the flux becomes confined to an increasingly thinner layer near the surface. Therefore, the subdivision thickness can be increased

$$\begin{aligned} Z &= \frac{2S}{I^2} \\ &= \frac{2\pi\alpha\left(\frac{4k(k-1)}{\pi\alpha} + [J_0(\alpha r_k)Y_1(\alpha r_{k-1}) - J_1(\alpha r_{k-1})Y_0(\alpha r_k)](k-1)^2 r_{k-1} + [J_0(\alpha r_{k-1})Y_1(\alpha r_k) - J_1(\alpha r_k)Y_0(\alpha r_{k-1})]\,k^2 r_k\right)}{\sigma l_s\,[J_0(\alpha r_{k-1})Y_0(\alpha r_k) - J_0(\alpha r_k)Y_0(\alpha r_{k-1})]}. \end{aligned} \tag{7}$$

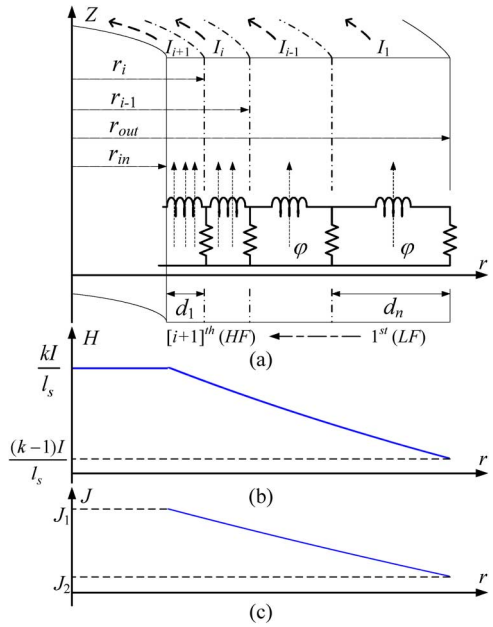

Fig. 4. (a) Dual Cauer circuit for the representation of eddy currents in nonuniformly laminated layer (kth layer individually represented), (b) magnetic field, and (c) current density distribution for $\omega = 0$.

from the inner surface toward the outer surface of the winding. For the single-layer winding depicted in Fig. 4, the boundary conditions are

$$H_z(r_{in}) = \frac{I}{l_s}, \quad H_z(r_{out}) = 0 \tag{14}$$

where $r_{\rm in}$ and $r_{\rm out}$ are the inner and outer radius of the layer, respectively. The magnetic field can be derived from (12) by substituting $k = 1$. The expressions for current density and total current in each section are

$$J = \nabla \times H = \frac{I}{l_s \ln\left(\frac{r_{\rm in}}{r_{\rm out}}\right) r} \tag{15}$$

$$I_i = \int_0^{l_s} \int_{r_i}^{r_{i-1}} J dz dr = \frac{\ln\left(\frac{r_{i-1}}{r_i}\right)}{\ln\left(\frac{r_{\rm in}}{r_{\rm out}}\right)} I := M_i I. \tag{16}$$

The curvature factor M_i is defined in (16), which accounts for the nonuniform distribution of the current (and flux) due to the cylindrical geometry selected for this paper. Equations (15) and (16) have been derived to calculate the current in each sublayer. This current is a function of the curvature of the winding and total current in the winding. It should be noted that this equation is derived for $\omega \to 0$; thus, there are no eddy currents induced. From (12) and (16), the inductance of each section is

$$L_{dc,i} = \frac{\mu\pi}{l_s \ln^2\left(\frac{r_{i-1}}{r_i}\right)} \times \left\{ \begin{array}{l} r_{i-1}^2 \left[\ln^2\left(\frac{r_{i-1}}{r_{out}}\right) - \ln\left(\frac{r_{i-1}}{r_{out}}\right) + 0.5\right] \\ -r_i^2 \left[\ln^2\left(\frac{r_i}{r_{out}}\right) - \ln\left(\frac{r_i}{r_{out}}\right) + 0.5\right] \end{array} \right\}. \tag{17}$$

The values of resistors are computed with the following simple expression:

$$R_i = \frac{l}{\sigma A} = \frac{2\pi r_{mean}}{\sigma l_s d} = \frac{\pi(r_{i-1} + r_i)}{\sigma l_s (r_{i-1} - r_i)}. \tag{18}$$

It is known that duality derived circuits frequently fail to properly represent the terminal behavior of the winding [16]. This is the case of the Cauer circuit of Fig. 4(a) when the parameters are computed with (17). The cause is that the proximity effects between sections are ignored. The proximity effect can be included in the model with mutual couplings between all subdivisions. This has been appropriate to represent proximity effects between different windings in [16] and [17]. However, for the single-layer conductor (or a multilayer winding) under investigation, it is not possible to excite subdivisions (or layers) independently. Thus, mutual couplings are meaningless in terms of representing the physical effects between subdivisions (or layers).

The values of the resistors to be entered in the Cauer model are those of (18). However, the dual/terminal inductors cannot be computed directly from (17). The fundamental modeling principle of this paper is that the equivalent inductance seen from the terminals of the Cauer circuit should be dual and simultaneously match the terminal behavior. Therefore, $L_{\rm eq} = {\rm Im}[Z_{{\rm eq},n}]/\omega = L_{\rm DC}$ when $\omega \to 0$; where $L_{\rm DC}$ is the inductance of the whole layer computed by (13) for $k = 1$. Two major effects prevent the inductors of (17) to satisfy duality and terminal behavior: 1) effect of curvature and 2) proximity effect. A method proposed here is to refine the inductance values considering the topology of the Cauer circuit to account for proximity and winding curvature effects. This method yields to the following equation (see details in Appendix A):

$$L_i = M_i^2 \left\{ \frac{\sum_{k=1}^{n} \left(\prod_{j=1, j\neq k}^{n} (R_j) \right)}{\sum_{k=i}^{n} \left(\prod_{j=1, j\neq k}^{n} (R_j) \right)} \right\}^2 L_{{\rm dc},i}. \tag{19}$$

The expression in brackets can be seen as a proximity effect factor; recall that M_i represents the effect of curvature. Resistors R_j could be substituted by corresponding values R_i, $i = 1, 2, \ldots, n$, presented in (18) yielding

$$L_i = M_i^2 \left\{ \frac{\sum_{k=1}^{n} \left(d_k \prod_{\substack{j=1 \\ j\neq k}}^{n} (r_{mean,j}) \right)}{\sum_{k=i}^{n} \left(d_k \prod_{\substack{j=1 \\ j\neq k}}^{n} (r_{mean,j}) \right)} \right\}^2 L_{{\rm dc},i} \tag{20}$$

where n is the number of subdivisions. Thus, all electrical parameters of the physical Cauer circuit are computed analytically from only the geometrical information and material properties of the transformer winding using (18) and (20) complemented by (17).

C. Optimization

Theoretically, models for eddy currents require an infinite number of sections to represent exactly the physical behavior of the windings. To achieve a given engineering accuracy over a finite frequency range, only a finite number of sections are sufficient for any existing model. The higher the desired accuracy and/or the wider the frequency range, the more sections are to be retained. A discretization pattern is presented in this section to obtain the optimum order of the circuit. Some essential physical constraints should be used: the sections under higher magnetic field (high-frequency region) should always be thinner than those of lower frequencies. Consequently, the width of the next sections should become progressively thicker. In addition, the width of the layer should be equal to the sum of the section thicknesses (d_i). These constraints are summarized as

$$d_1 \leq d_2 \ldots\ldots \leq d_n; \quad d = \sum_{i=1}^{n} d_i. \tag{21}$$

For a circuit consisting of n sections, the thickness d_i could be varied with a constant step Δd. The minimum possible thickness $d_{\min}$ is taken as Δd in this paper. The following expression (in pseudo Matlab code) examines all possible subdivisions to obtain the optimal discretization:

$$\begin{aligned} d_1 &= d_{\min} : \Delta d : d/n \\ d_2 &= d_1 : \Delta d : (d - d_1)/(n-1) \\ &\vdots \\ d_{n-1} &= d_{n-2} : \Delta d : \left(d - \sum_{i=1}^{n-2} d_i \right) /2 \\ d_n &= d - \sum_{i=1}^{n-1} d_i. \end{aligned} \tag{22}$$

$\Delta d = 0.01$ mm is considered to be a portion of penetration depth $\delta (\approx 0.07$ mm) in a copper winding at a maximum frequency of 1 MHz. The optimization is performed to minimize the following error function:

$$e(\%) = \frac{100}{2n_\omega} \sum_{i=1}^{n_\omega} \left(\left| \frac{R_{\mathrm{FEM},i} - R_{\mathrm{Model},i}}{R_{\mathrm{FEM},i}} \right| + \left| \frac{L_{\mathrm{FEM},i} - L_{\mathrm{Model},i}}{L_{\mathrm{FEM},i}} \right| \right) \tag{23}$$

where $n_\omega = 81$ corresponds to the total number of fitting frequencies (10^{-2} to 10^6 Hz in a logarithmic scale). Simulation results show that the solutions are independent of r_{in}. Results are only functions of the maximum frequency $f_{\max}$ and the overall thickness d. Therefore, the maximum frequency of interest should be selected first. For low-frequency transient studies $f_{\max} = 3$ kHz [18], for a slow-front transient $f_{\max} = 10$ kHz [5], and for fast-front transients $f_{\max} = 1$ MHz [19], are recommended. The thickness of the layer d is varied from 1 to 10 mm. The maximum value of d is selected as 10 mm, close to the penetration depth of copper at the rated frequency.

TABLE I
PERCENTAGE OF SUBDIVISION THICKNESSES FOR LOW-FREQUENCY TRANSIENTS

k	d (mm)									
	1	2	3	4	5	6	7	8	9	10
1	100	100	100	16.0	16.4	11.1	10.1	6.9	6.2	5.9
2	-	-	-	84.0	83.6	13.5	12.7	8.1	7.8	7.6
3	-	-	-	-	-	75.4	77.2	11.6	12.1	12.0
4	-	-	-	-	-	-	-	73.4	73.9	74.5
Sum	100	100	100	100	100	100	100	100	100	100
ε %	0.1	1.2	3.7	4.0	5.2	4.2	4.8	4.0	4.4	4.9

TABLE II
PERCENTAGE OF SUBDIVISION THICKNESSES FOR SLOW FRONT TRANSIENTS

k	d (mm)									
	1	2	3	4	5	6	7	8	9	10
1	100	16.0	11.3	9.7	6.0	4.5	4.1	3.1	2.9	2.7
2	-	84.0	13.3	12.7	7.6	5.3	5.0	3.5	3.3	3.1
3	-	-	75.4	77.6	12.0	7.5	7.0	4.5	4.2	4.0
4	-	-	-	-	74.4	11.5	11.1	6.3	6.1	6.0
5	-	-	-	-	-	71.2	72.8	10.4	10.3	10.2
6	-	-	-	-	-	-	-	72.2	73.2	74
Sum	100	100	100	100	100	100	100	100	100	100
ε %	1.0	3.6	3.8	4.9	4.4	4.1	4.6	4.2	4.5	4.9

IV. RESULTS AND DISCUSSION

In the following subsections, the implementation of the model for various transient studies is described.

A. Low-Frequency Transients

This category includes studies, such as load rejection, inrush currents (transformer energization), harmonic interactions, temporary overvoltages, and ferroresonance [18].

The optimal thickness of the divisions as a percent of conductor thickness is presented in Table I. In this table, k stands for the section number. The results presented in Table I show that for low-frequency transients, a circuit with four sections is sufficient even for a 10-mm-thick conductor with a maximum relative error of less than 5%.

For thinner conductors, the penetration depth for maximum frequency is larger than the conductor itself. Thus, frequency-dependent modeling is unnecessary. These cases correspond to columns one to three in Table I.

From columns 4 to 10 of Table I, one can observe that for thicker conductors ($d > 4$ mm), it is necessary to represent the eddy current effects with a multisection model to keep the error under 5%. Traditional low-frequency models (using a resistance and an inductance) may produce large errors.

B. Slow Front Transients

This is the case of transient phenomena well below the first winding resonance. They include most switching transients, magnetizing current chopping (transformer de-energization), transient recovery voltage (fault clearing), and fault initiations [5]. The optimal results are presented in Table II. For slow front transients, a circuit with a maximum order of six sections gives acceptable accuracy.

C. Fast-Front Transients

This case is for lightning transients and impulse test studies to design insulation systems [19]. For these transients, good ac-

TABLE III
PERCENTAGE OF SUBDIVISION THICKNESSES FOR FAST FRONT TRANSIENTS

k	d (mm)									
	1	2	3	4	5	6	7	8	9	10
1	3.0	1.5	0.7	0.5	0.4	0.3	0.3	0.3	0.2	0.3
2	4.0	1.5	1	0.5	0.4	0.3	0.3	0.3	0.3	0.3
3	5.0	2.0	1	0.5	0.4	0.3	0.4	0.4	0.3	0.4
4	10.0	3.5	1.3	0.7	0.6	0.5	0.4	0.4	0.4	0.5
5	78.0	6.0	2.3	1.0	0.8	0.7	0.7	0.6	0.7	0.7
6	-	11.0	3.7	1.5	1.2	1.0	1.0	1.0	1.0	1.1
7	-	74.5	6.3	2.5	1.8	1.7	1.6	1.6	1.6	1.6
8	-	-	11	4.0	2.8	2.7	2.6	2.5	2.4	2.6
9	-	-	72.7	6.5	4.3	4.0	4.0	4.0	3.8	3.9
10	-	-	-	11.2	6.7	6.4	6.3	6.4	6.2	6.4
11	-	-	-	71.1	11.5	11.1	10.9	11.1	10.8	11.0
12	-	-	-	-	69.1	71.0	71.5	71.4	72.3	71.2
Sum	100	100	100	100	100	100	100	100	100	100
ε %	4.5	4.9	4.8	4.5	4.4	4.8	5.2	5.5	5.7	6

TABLE IV
CURRENT FLOWING THROUGH THE SECTIONS. FEM VERSUS CURRENT IN THE MODEL RESISTANCES SIMULATED WITH THE EMTP (%)

Frequency		1st	2nd	3rd	4th	5th
10 kHz	FEM	35.07	26.36	20.46	13.04	5.07
	EMTP	36.52	27.47	20.42	12.84	2.75
3 kHz	FEM	22.00	20.30	20.60	19.49	17.61
	EMTP	22.04	20.72	21.30	21.07	14.87
1 kHz	FEM	14.18	14.54	16.91	19.50	34.87
	EMTP	14.25	14.63	16.69	18.00	36.43

curacy could be obtained with a maximum of 12 sections using the percent values presented in Table III.

D. Flux and Current in Windings

According to the principle of duality a one-to-one relationship exists not only between the topology of the circuit and the construction elements of the electromagnetic device, but also between the electrical parameters in the model and the physical behavior of the device [20]. For example, the current flow in each section corresponds to the current of the relevant resistance in the model. Then, the magnetic flux φ_i in each section can be calculated from [20]

$$\phi_i = L_i I_i \tag{24}$$

where I_i is the current of the ith inductor L_i. For validation, a case study has been developed for a conductor with $d = 6$ mm and frequencies up to 10 kHz. The parameters are calculated according to the 6th column of Table II. The current and flux in the different sections are presented in Tables IV and V, respectively. The values are presented in percent of the total current and total flux in each case.

One can appreciate from Tables IV and V that the differences between the currents and fluxes computed with FEM and those computed with the Physical Cauer model (EMTP) are small in general. The differences in columns 1st to 4th are under 4%. Larger differences occur in the 5th column, which means that a model of a higher order should be selected when higher precision in the magnitude of the eddy currents is required.

TABLE V
MAGNETIC FLUX IN THE SECTIONS. FEM VERSUS MODEL WITH EMTP SIMULATIONS (%)

Frequency		1st	2nd	3rd	4th	5th
10 kHz	FEM	34.09	25.70	20.14	13.16	6.91
	EMTP	33.38	25.31	20.54	13.87	6.90
3 kHz	FEM	20.60	19.03	19.37	18.47	22.53
	EMTP	20.75	19.06	19.29	17.83	23.07
1 kHz	FEM	13.16	13.49	15.73	18.36	39.26
	EMTP	13.50	13.82	16.19	19.43	37.06

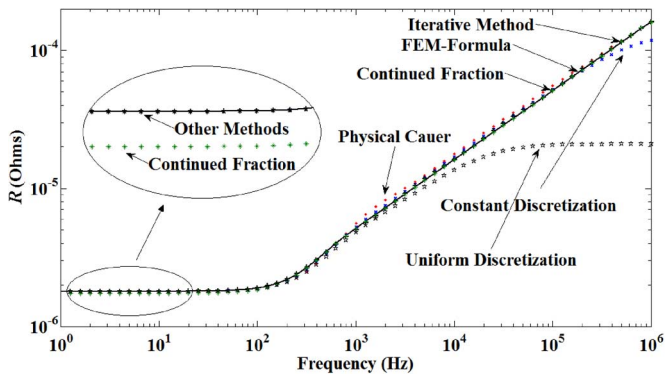

Fig. 5. Frequency response of resistance ($d = 6$ mm, $r_{in} = 10$ mm, $l_s = 1$ m).

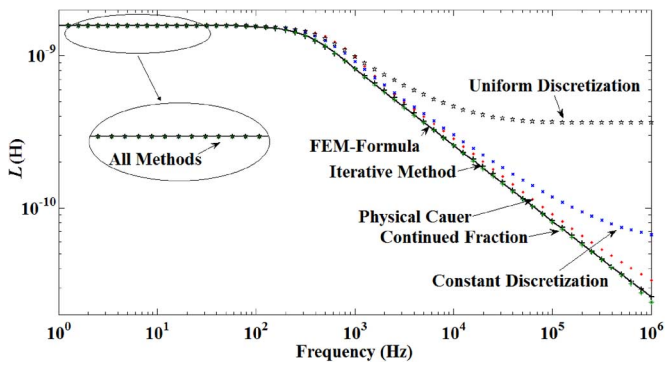

Fig. 6. Frequency response of inductance ($d = 6$ mm, $r_{\rm in} = 10$ mm, $l_s = 1$ m).

E. Model Comparison and Discussions

For comparison, a case with $d = 6$ mm and a maximum frequency of 1 MHz is simulated; the variations in the electrical parameters with frequency are presented in Figs. 5 and 6. The physical Cauer model proposed in this paper is compared with a few available modeling alternatives, such as impedances obtained from the formula, uniform domain discretization method, constant discretization method, iterative technique, and continued fraction model. The information regarding the aforementioned models is presented in Appendix B. All equivalent circuits are represented with 12 sections except for the iterative method (eight sections). This method gives good accuracy with a smaller order than the other methods, but it does not permit full physical interpretation, in the dual sense, as the physical Cauer model does.

Continued fraction models are analytically ideal because they are derived directly from the mathematical impedance formula. The model is unique according to the continued fraction expansion of the field solution equation. But the accuracy is dependent on the accuracy of the analytical formula. In our case, the exact formula (7) does not have a continued fraction expansion. Thus, the approximate formula (10) has been used, which is not accurate for resistances at lower frequencies. At lower frequencies, the approximate formula has an error of about 5%. As discussed before, the continued fraction circuit is a terminal model with no physical significance.

Both uniform and nonuniform discretization methods discussed in this paper are physical. Uniform discretization is less accurate than incremental discretization with a constant ratio. However, the main drawback of the constant incremental discretization method is that for different cases, different ratios give the best results.

V. Conclusion

A physical Cauer circuit has been proposed to model the eddy current effects in transformer windings. The model has been developed from the solution of the electromagnetic-field problem in dc and accurately predicts the behavior of inductance and resistance for frequencies of up to 1 MHz. The parameters of the optimal model are computed from simple and efficient formulas [(17), (18), and (20)] that rely only on geometrical information. It has been confirmed that the electrical model is completely dual to the electromagnetic phenomena with finite-elements simulations. The current in the inductors is analogous to the magnetic flux, while currents flowing in the winding sections correspond to currents in the model's resistors. Therefore, the circuit can give a precise and accurate view of the electromagnetic phenomena occurring in the windings.

This paper is a continuation of previous work presented in [16] and [17] aimed to create a completely dual transformer model for the calculation of electromagnetic transients. The techniques in the paper are valid for a solid single-layer winding up to at least 1 MHz which is well below the quasistatic limit for a single copper conductor. The effect of capacitances will be presented in an upcoming paper for multilayer windings and multiwinding transformers. The model has been only applied to layer windings. However, it is believed that the same methodology can be applied to disks.

Appendix A
Calculation of Circuit Parameters

The objective of this section is to obtain the correct inductance values for each layer in the circuit, such that the model is fully dual and matches the terminal behavior. Two refinements of the inductance parameters $L_{dc,i}$ of (17) are required to satisfy the following modeling principle: $L_{eq} = \mathrm{Im}[Z_{eq,n}]/\omega = L_{DC}$ when $\omega \to 0$. The first step is to account for the effect of curvature. Assume that in a single layer a total current I flows, according to (16), the current in the i^{th} section is $I_i = M_i I$. The total magnetic energy W produced by I is computed by superposition of the magnetic energy caused by all section currents I_i. Then new parameters $L'_{\mathrm{dc},i} = M_i^2 L_{\mathrm{dc},i}$ are introduced

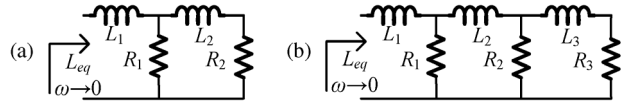

Fig. 7. Physical Cauer Circuits. (a) Order two. (b) Order three.

$$\begin{aligned} L_{\mathrm{DC}} &= \frac{2W}{I^2} = \frac{2(W_1 + W_2 + \cdots W_n)}{I^2} \\ &= \frac{2W_1}{I^2} + \frac{2W_2}{I^2} + \cdots \frac{2W_n}{I^2} \\ &= M_1^2 L_{dc,1} + M_2^2 L_{dc,2} + \cdots M_n^2 L_{dc,n} \\ &= L'_{\mathrm{dc},1} + L'_{dc,2} + \cdots L'_{dc,n} \end{aligned} \tag{25}$$

Circuit topology causes the terminal inductance at dc (L_{eq}) to become different from L_{DC} because it considers proximity effects. Thus, parameters $L'_{\mathrm{dc},i}$ should be modified to obtain the correct L_i. For this reason, low-frequency inductances seen at the terminals of order two and order three Physical Cauer circuits (depicted in Fig. 7) are computed from $L_{\mathrm{eq},n} = \mathrm{Im}[Z_{\mathrm{eq},n}]/\omega$ when $\omega \to 0$, yielding

$$L_{\mathrm{eq},2} = L_1 + \frac{R_1^2 L_2}{(R_1 + R_2)^2} \tag{26a}$$

$$L_{\mathrm{eq},3} = L_1 + \frac{(R_1R_2 + R_1R_3)^2 L_2 + (R_1R_2)^2 L_3}{(R_1R_2 + R_1R_3 + R_2R_3)^2}. \tag{26b}$$

For a circuit with one section $L_1 = L_{\mathrm{eq},1} = L_{\mathrm{DC}} = L'_{\mathrm{dc},1} = L_{\mathrm{dc},1}$; for a circuit with two sections $L_{\mathrm{eq},2} = L_{\mathrm{DC}} = L'_{\mathrm{dc},1} + L'_{\mathrm{dc},2}$; for a circuit with three sections $L_{\mathrm{eq},3} = L_{\mathrm{DC}} = L'_{\mathrm{dc},1} + L'_{\mathrm{dc},2} + L'_{\mathrm{dc},3}$ and so forth. Thus, according to (26a), the following relationships for circuits with two sections can be written:

$$\begin{aligned} L_1 &= L'_{\mathrm{dc},1} \Rightarrow L_1 = M_1^2 L_{\mathrm{dc},1} \\ L_2 &= \frac{(R_1 + R_2)^2}{R_1^2} L'_{\mathrm{dc},2} \Rightarrow L_2 \\ &= M_2^2 \frac{(R_1 + R_2)^2}{R_1^2} L_{\mathrm{dc},2}. \end{aligned} \tag{27a}$$

Following the same procedure for a circuit with three sections, we have:

$$\begin{aligned} L_1 &= M_1^2 L_{\mathrm{dc},1} \\ L_2 &= M_2^2 \frac{(R_1R_2 + R_1R_3 + R_2R_3)^2}{(R_1R_2 + R_1R_3)^2} L_{\mathrm{dc},2} \\ L_3 &= M_3^2 \frac{(R_1R_2 + R_1R_3 + R_2R_3)^2}{(R_1R_2)^2} L_{\mathrm{dc},3}. \end{aligned} \tag{27b}$$

Equation (19) is the generalization of the above pattern.

APPENDIX B
RESISTORS AND INDUCTORS OF FIG. 1

In this section, expressions for the calculation of the resistors and inductors of the two kinds of Cauer models in Fig. 1 by means of other commonly used methods are given. The reason to include them here is that they are not published anywhere and would help a reader to reproduce our results.

A. Continued Fraction Model

The approximate formula (10) is developed in continued fractions. The values of the equivalent circuit parameters are:

$$L_k = \frac{2\pi\mu d r_k}{(4k-1)l_s}, \quad R_k = \frac{(8k-6)\pi r_k}{\sigma l_s d}, \quad k = 1, 2, \ldots n. \tag{28}$$

B. Physical Cauer-Iterative Method

Parameter values G_i (conductance corresponding to R_i) and L_i $(i = 1, 2, \ldots n)$ are fitted with frequencies ω_i. Z_{ir} and Z_{il} are the impedances, seen from the right and left side of block i, respectively. According to the procedure described in [1], the following equations are derived for the physical Cauer circuit, which should be solved iteratively

$$-C\left(L_{ir}^2\omega_i^2 + R_{ir}^2\right)G_i^2 + \left(R_{ir}^2 + L_{ir}^2\omega_i^2 - 2R_{ir}C\right)G_i + R_{ir} - C = 0 \tag{29}$$

$$\mathrm{Im}\left(Z_{il}(\omega_i)\right) = \omega_i L_i + \omega_i L_{ir} / \left[\left(1 + G_i R_{ir}\right)^2 + \left(G_i L_{ir}\omega_i\right)^2\right] \tag{30}$$

where $C = \mathrm{Re}[Z_{il}(\omega_i)]$. For the innermost block, which is dedicated to lower frequencies, the following equations are used:

$$G_i = \left[\mathrm{Re}\left(Z_{il}(\omega_i)\right)\right]^{-1}, \quad L_i = \omega_i^{-1}\mathrm{Im}\left(Z_{il}(\omega_i)\right). \tag{31}$$

REFERENCES

[1] F. de León and A. Semlyen, "Time domain modeling of eddy current effects for transformer transients," *IEEE Trans. Power Del.*, vol. 8, no. 1, pp. 271–280, Jan. 1993.

[2] F. de León and A. Semlyen, "Detailed modeling of eddy current effects for transformer transients," *IEEE Trans. Power Del.*, vol. 9, no. 2, pp. 1143–1150, Apr. 1994.

[3] A. Semlyen and F. de León, "Eddy current add-on for frequency dependent representation of winding losses in transformer models used in computing electromagnetic transients," *Proc. Inst. Elect. Eng., Gen. Transm. Distrib.*, vol. 141, pp. 209–214, May 1994.

[4] J. A. Martínez, R. Walling, B. Mork, J. Martin-Arnedo, and D. Durbak, "Parameter determination for modeling systems transients. Part III: Transformers," *IEEE Trans. Power Del.*, vol. 20, no. 3, pp. 2051–2062, Jul. 2005.

[5] J. A. Martínez and B. A. Mork, "Transformer modeling for low and mid-frequency transients—A review," *IEEE Trans. Power Del.*, vol. 20, no. 2, pt. 2, pp. 1625–1632, Apr. 2005.

[6] F. de León, "Transformer modeling for low and mid-frequency transients–A review," *IEEE Trans. Power Del.*, vol. 23, no. 2, pp. 1625–1632, Apr. 2008.

[7] J. H. Krah, "Optimum discretization of physical cauer circuit," *IEEE Trans. Magn.*, vol. 41, no. 5, pp. 1444–1447, May 2005.

[8] P. Holmberg, "Modeling the transient response of windings, laminated steel cores and electromagnetic power devices by means of lumped circuits," Ph.D. dissertation, Inst. High Voltage Res., Uppsala University, Uppsala, Sweden, 2000.

[9] P. Holmberg, M. Leijon, and T. Wass, "A wideband lumped circuit model of eddy current losses in a coil with a coaxial insulation system and a stranded conductor," *IEEE Trans. Power Del.*, vol. 18, no. 1, pp. 50–60, Jan. 2003.

[10] F. de León, "A wideband lumped circuit model of eddy current losses in a coil with a coaxial insulation system and a stranded conductor," *IEEE Trans. Power Del.*, vol. 19, no. 2, p. 902, Apr. 2004.

[11] P. G. Blanken, "A lumped winding model for use in transformer models for circuit simulation," *IEEE Trans. Power Electron.*, vol. 16, no. 3, pp. 445–460, May 2001.

[12] G. C. Temes and J. W. Lapatra, *Introduction to Circuit Synthesis and Design*. New York: McGraw-Hill, 1997.

[13] J. Lammeraner and M. Stafl, *Eddy Currents*. Boca Raton, FL: CRC, 1966.

[14] M. Perry, *Low Frequency Electromagnetic Design*. New York: Marcel Dekker, 1985.

[15] M. Abramowitz and I. A. Stegun, *Handbook of Mathematical Functions-With Formulas, Graphs, and Mathematical Tables*. New York: Dover, 1970.

[16] C. Álvarez-Mariño, F. de León, and X. M. López-Fernández, "Equivalent circuit for the leakage inductance of multi-winding transformers: Unification of terminal and duality models," *IEEE Trans. Power Del.*, vol. 27, no. 1, pp. 353–361, Jan. 2012.

[17] F. de León and J. A. Martinez, "Dual three-winding transformer equivalent circuit matching leakage measurements," *IEEE Trans. Power Del.*, vol. 24, no. 1, pp. 160–168, Jan. 2009.

[18] J. C. Das, *Transients in Electrical Systems: Analysis, Recognition, and Mitigation*. New York: McGraw-Hill Prof Med/Tech, 2010.

[19] Fast Front Transients Task Force of the IEEE. Modeling and Analysis of System Transients. Working Group, "Modeling guidelines for fast front transients," *IEEE Trans. Power Del.*, vol. 11, no. 1, pp. 493–506, Jan. 1996.

[20] G. R. Slemon, *Electric Machines and Drives*. Reading, MA: Addison-Wesley, 1992.

Saeed Jazebi (S'10) was born in Kerman, Iran, in 1983. He received the B.Sc. degree in electrical engineering from Shahid Bahonar University, Kerman, in 2006, the M.Sc. degree in electrical engineering from Amirkabir University of Technology, Tehran, Iran, in 2008, and is currently pursuing the Ph.D. degree in electrical engineering at the Polytechnic Institute of New York University, Brooklyn, NY.

His fields of interest include electromagnetic design, modeling, and simulation of electrical machines and power system components; statistical pattern-recognition applications in power engineering; power system protection; and power quality.

Francisco de León (S'86–M'92–SM'02) received the B.Sc. and M.Sc. (Hons.) degrees in electrical engineering from the National Polytechnic Institute, Mexico City, Mexico, in 1983, and 1986, respectively, and the Ph.D. degree in electrical engineering from the University of Toronto, Toronto, ON, Canada, in 1992.

He has held several academic positions in Mexico and has worked for the Canadian electric industry. Currently, he is an Associate Professor at the Polytechnic Institute of New York University, Brooklyn, NY. His research interests include the analysis of power definitions under nonsinusoidal conditions, the transient and steady-state analyses of power systems, the thermal rating of cables and transformers, and the calculation of electromagnetic fields applied to machine design and modeling.

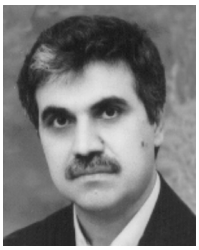

Behrooz Vahidi (M'00–SM'04) was born in Abadan, Iran, in 1953. He received the B.S. degree in electrical engineering from Sharif University of Technology, Tehran, Iran, in 1980, the M.S. degree in electrical engineering from Amirkabir University of Technology, Tehran, Iran, in 1989, and the Ph.D. degree in electrical engineering from the University of Manchester Institute of Science and Technology Manchester, U.K., in 1997.

From 1980 to 1986, he worked in the field of high voltage in industry as Chief Engineer. Since 1989, he has been with the Department of Electrical Engineering, Amirkabir University of Technology , where he is currently a Professor. His main fields of research are high voltage, electrical insulation, power system transients, lightning protection, and pulse power technology.